NERC Open Research Archive
*sharing our research*

Centre for
Ecology & Hydrology
NATURAL ENVIRONMENT RESEARCH COUNCIL

## Article (refereed) - postprint

1 **Process-based simulation of growth and overwintering of grassland using the**
2 **BASGRA model**

3 Mats Höglind[1*], Marcel Van Oijen[2], David Cameron[2], Tomas Persson[1]

4 [1]Norwegian Institute of Bioeconomy Research, 4353 Klepp stasjon, Norway
5 [2]CEH-Edinburgh, Bush Estate, Penicuik EH26 0QB United Kingdom
6
7 *Corresponding author: Tel. +4740475391
8 E-mail addresses: mats.hoglind@nibio.no (M. Höglind), mvano@ceh.ac.uk (M. Van Oijen),
9 dcam@ceh.ac.uk (D. Cameron), tomas.persson@nibio.no (T. Persson)

10 **Abstract**

11 Process-based models (PBM) for simulation of weather dependent grass growth can assist
12 farmers and plant breeders in addressing the challenges of climate change by simulating
13 alternative roads of adaptation. They can also provide management decision support under
14 current conditions. A drawback of existing grass models is that they do not take into account the
15 effect of winter stresses, limiting their use for full-year simulations in areas where winter
16 survival is a key factor for yield security. Here, we present a novel full-year PBM for grassland
17 named BASGRA. It was developed by combining the LINGRA grassland model (Van Oijen et
18 al. 2005) with models for cold hardening and soil physical winter processes. We present the
19 model and show how it was parameterized for timothy (*Phleum pratense* L.), the most important
20 forage grass in Scandinavia and parts of North America and Asia. Uniquely, BASGRA simulates
21 the processes taking place in the sward during the transition from summer to winter, including
22 growth cessation and gradual cold hardening, and functions for simulating plant injury due to
23 low temperatures, snow and ice affecting regrowth in spring. For the calibration, we used
24 detailed data from five different locations in Norway, covering a wide range of agroclimatic
25 regions, day lengths (latitudes from 59° to 70° N) and soil conditions. The total dataset included
26 11 variables, notably above-ground dry matter, leaf area index, tiller density, content of C
27 reserves, and frost tolerance. All data were used in the calibration. When BASGRA was run with
28 the maximum a-posteriori (MAP) parameter vector from the single, Bayesian calibration, nearly
29 all measured variables were simulated to an overall normalized root mean squared error
30 (NRMSE) < 0.5. For many site x experiment combinations, NRMSE was < 0.3. The temporal
31 dynamics were captured well for most variables, as evaluated by comparing simulated time
32 courses vs. data for the individual sites. The results may suggest that BASGRA is a reasonably
33 robust model, allowing for simulation of growth and several important underlying processes with

acceptable accuracy for a range of agroclimatic conditions. However, the robustness of the model needs to be tested further using independent data from a wide range of growing conditions. Finally we show an example of application of the model, comparing overwintering risks in two climatically different sites, and discuss future model applications. Further development work should include improved simulation of the dynamics of C reserves, and validation of winter tiller dynamics against independent data.

# 1 Introduction

## 1.1 Grasslands and climate change

Grasslands constitute the most important source of energy and nutrients for grazing animals in large regions of the world. In temperate and boreal regions, where low temperatures restrict or prevent growth during winter, grasslands are also extremely important for the production of conserved forage for winter feeding of cattle, sheep, goats and horses. Grass-based dairy and meat production constitute the economic backbone of agriculture in Northern Europe including Norway. Timothy (*Phleum pratense* L.) is the most important forage grass in Scandinavia and parts of North America and Asia where winter survival is critical. Compared to perennial ryegrass (*Lolium perenne* L.), which is grown in areas with milder winter conditions, timothy is more tolerant to most winter stresses (Höglind et al, 2010). However, weather driven inter-annual variation in grass yields may lead to substantial variation in the economic output of forage based livestock production even in systems where timothy is the dominant grass species.

Grassland productivity is expected to be affected by climate change (Tubiello et al. 2007; Jing et al. 2014). The changes may be detrimental or, especially at high latitudes, beneficial. However, there is still large uncertainty with respect to grassland productivity in Northern Europe under future climate conditions (Höglind et al. 2013). There is a lack of knowledge especially about the impact of weather conditions late in the growing season and during the winter on the inter-survival of the tillers, and thus the regrowth and yield of the sward. Increases in temperature variability may lead to warm spells that interrupt winter hardening and make the plants more sensitive to subsequent frost (Bélanger et al. 2002, Rapacz et al. 2014). The survival rate will not depend on the winter climate alone, but also on the state of the sward itself during the transition

64  from growing season to winter, which in turn is affected by the environmental conditions during

65  the growing season, sward genotype and management. Farmers can adapt to climate change by

66  choosing different grass species or cultivars and by adjusting management practices such as

67  fertilizer application strategies and timing of harvests. Plant breeders can contribute to the

68  adaptation of climate change by breeding grasses that grow well under expected conditions.

69  **1.2 Strengths and weaknesses of existing grassland models**

70  Process-based models for weather dependent grass growth can assist farmers and plant breeders

71  in the process of adaptation to climate change by simulating different adaptation options. These

72  models can also be used to investigate different management options such as the prediction of

73  the optimal harvest time for use in tactical planning at farm level under current conditions

74  (Bonesmo and Belanger, 2002). A number of process-based grassland models for cold temperate

75  climate conditions including LINGRA (Schapendonk et al. 1998; Höglind et al. 2001; Van Oijen

76  et al. 2005a), the Hurley pasture model (Thornley and Cannell 1997), PaSIM (Riedo et al. 1998),

77  CATIMO (Bonesmo and Bélanger, 2002), and STICS (Jégo et al. 2013) are available for use in

78  this type of studies. A common feature for all the available grassland models is that they

79  simulate the accumulation of biomass as dependent on temperature and the availability of light

80  and water. Many models also simulate the effect of nutrient availability on grass growth and

81  quality (e.g. Bonesmo and Bélager, 2002; Jégo et al. 2013). However, nearly all the existing

82  grassland models for temperate climate conditions focus exclusively on the spring and summer

83  growing season. Hence they cannot be used for predicting winter survival, which limits their

84  usefulness for predicting grassland productivity in regions where winter survival is critical. An

85  exception is the PaSIM model (Riedo et al. 1998) that simulates snow cover dynamics and the

86  effect of snow cover on the temperature around the plant. However, this model does not simulate

87  ice-cover and does not take into account the effects of cold stress, limiting its usefulness to

88  winter conditions that constitute no risk to tiller survival.

89  **1.3 Development of the new model BASGRA**

90  Here, we present a full-year model for grassland growth named Basic Grassland Model

91  (BASGRA), and parameterise it for timothy. It was developed by combining the LINGRA

92  grassland model as used for summer growth of timothy (Van Oijen et al. 2005a) with the model

93  for cold hardening and dehardening in grasses developed by Thorsen and Höglind (2010), and

94  the SnowFrostIce model for soil physical winter processes in grasslands (Thorsen et al. 2010)

95  with some modifications of the original models and some additional functions to handle the

96  transition between summer and winter. Growth in BASGRA is modelled as dependent on

97  source-sink relationships, which affect the dynamics of tiller density and leaf area in a similar

98  way as in its forerunner LINGRA. Modifications of the original model include additional control

99  functions for tillering, leaf appearance and leaf elongation, and a new algorithm for carbon

100 allocation. Other novel aspects of the BASGRA model are:

101     o  full-year simulation with different links between sward management, weather,
102        day length, soil physics and plant ecophysiology,
103     o  mechanistic simulation of the processes taking place in the sward during the
104        transition from summer to winter including growth, cessation, the build-up of
105        carbon reserves and the gradual frost hardening of the plants,
106     o  comprehensive representation of winter damage processes related to low
107        temperatures, short days with low irradiation, snow- and ice-covered fields
108     o  mechanistic simulation of the resumption of growth in spring,
109     o  inclusion of a third tiller category: non-elongated generative tillers.

110 For each of the models that were combined to form BASGRA, similar design principles were

111 followed. Model structure was intended to allow simulation of the behaviour of the grass-soil

112 system in different growing environments, with different possible disturbances. Moreover, we

113 intended to simulate both short- and long-term responses to disturbances, so state variables

114 needed to be included that determine a sward's capacity to regrow, such as carbohydrate reserves

115 and tiller density. These objectives led to a fairly long list of model processes, as outlined above,

116 and as described in detail in section 2. At the same time, the intention was to keep model

117 structure as simple as possible, such that it would be possible to collect sufficient data for model

118 parameterisation and for testing at the level of the represented processes. Where possible,

119 parameter-sparse process representations were chosen, e.g. a canopy light-use efficiency (LUE)

120 approach rather than a leaf photosynthesis model, but with LUE not treated as a constant to

121 allow for sward responses to changes in the availability of water and $CO_2$.

122 **1.4 Aims and outline of the remainder of this paper.**

123 The major aim of this paper is to present the BASGRA model and show how it was

124 parameterized. A second aim is to show an example of model application, and to discuss the

125 scope for future applications. We first present, in Section 2, the details of the model structure.

126 The focus is on features that are unique to BASGRA, and that have not been presented in detail
127 before. We then show in Section 3 how the model was parameterised, with emphasis on
128 parameters not usually part of grassland models. In Section 4, we show an example application
129 of the model to multi-year simulation of timothy growth at two sites in Norway. The paper is
130 concluded with a discussion of the modelling approach and an outlook of future applications.

# 2 Model structure

## 2.1 Model overview

133 The grassland model BASGRA is a mechanistic model for simulating the year-round dynamics
134 of tillers, leaves, roots and reserves. The model simulates the response of the sward to soil
135 conditions, cutting, day length, and the weather including winter stresses. The model operates at
136 a daily time step and contains 23 state variables and 71 initial constants and other parameters.

137 The three main features that characterize plant growth in BASGRA are: (1) simulation of source-
138 sink relations where the source consists both of current photosynthesis and remobilisation of
139 reserves, (2) simulation of leaf area dynamics and tillering for vegetative and generative tillers;
140 and (3) cold hardening and the effect of physical winter stress factors on tiller survival and plant
141 growth. Inputs to the model are daily values of radiation, temperature, rain, humidity and wind.
142 The soil is characterised by a soil water retention curve, initial soil water content and soil
143 temperature. In addition to the water balance, the depth of snow and ice on the soil surface as
144 well as the temperature at the soil surface and the depth of frost in the soil are simulated.

145 Photosynthesis is sensitive to light intensity, temperature, day length, $CO_2$ concentration and
146 water availability. Carbon from photosynthesis and remobilised reserves is allocated between
147 sinks according to a system of changing sink priorities and changing sink strengths. Sink
148 strengths are determined by the dynamics of leaves and stems and the acclimation to low
149 temperature. The major occasional disturbance during the growing season is removal of tillers
150 and leaves by cutting, with subsequent regrowth of the sward. Regrowth rate after cutting
151 depends on the phenological stage at which cutting take place and on the strengths of sources
152 and sinks. Damage by frost and by anaerobic conditions under ice accelerates senescence
153 depending on the degree to which the plants are hardened. BASGRA is a one-dimensional model
154 in that it keeps track of the height of snow cover and the depth to which the soil is frozen and
155 roots are grown. The model does not simulate nitrogen relations or plant disease impact.

156    BASGRA is implemented in open source software; Fortran and R. The model version presented

157    here, BASGRA 2014, is achieved online at http://dx.doi.org/10.5281/zenodo.27867 from where

158    full code, including for Bayesian calibration, can be downloaded as a zip-file (Van Oijen et al.,

159    2015). The zip-file also contains a comprehensive User Guide (including lists of parameters and

160    variables with names and units, and conceptual diagrams of the model) and all the necessary files

161    to run the model for default conditions (for cultivar Grindstad grown at Særheim in Norway) or

162    to apply Bayesian calibration to the model parameters (one example using observations of

163    Grindstad grown at Særheim). The User Guide also explains the history of the model.

164    In the following sections, we describe the major functions of BASGRA in more detail, with

165    focus on the functions that are unique for the BASGRA model, and how it differs from its three

166    predecessors, the LINGRA model for summer growth of timothy (Höglind et al. 2001; Van

167    Oijen et al. 2005a), the model for cold hardening in timothy (Thorsen and Höglind, 2010), and

168    the SnowFrostIce model for physical soil processes during the winter (Thorsen et al. 2010).

## 2.2 Soil processes and links to plant processes

170    The soil module of BASGRA combines the soil-water balance model for non-frozen summer

171    conditions used in LINGRA (Höglind et al. 2001) with the SnowFrostIce model that simulates

172    freezing and thawing in the soil (Thorsen et al. 2010). Both models have been described in detail

173    in the cited works; their major features are summarized below.

174    Soil water and above-ground non plant bound water in the form of snow and ice in BASGRA is

175    characterized by eight state variables. Two are spatial variables, representing snow cover height

176    and soil frost depth. The remaining six state variables represent the mass of water in different

177    phases (liquid, snow, ice) and locations (above- and belowground). During the growing season,

178    all water states, except for the state variable representing the mass of liquid water in the soil,

179    tend to be zero. BASGRA then acts as a model with a single soil layer between surface and

180    rooting depth. Water is added to the soil pool by rain and irrigation, and by root growth leading

181    to exploration of deeper soil. Water is lost from the soil through drainage, runoff, evaporation

182    and transpiration by plants. Water availability to plants is determined by rooting depth and the

183    amount of plant available water in that zone.

184

185    The form of precipitation is determined by a threshold temperature. Below the threshold,

186    precipitation falls as snow, adding to the state variables representing mass of snow per unit

187 ground area and the height of the snow pack. If the soil surface temperature falls below the

188 freezing point, soil water will start freezing from the top. This is captured by a state variable for

189 the mass of ice in the soil and a state variable for the depth of the ice layer. Once frost depth

190 exceeds a threshold of 0.2 m, it is assumed that liquid water no longer infiltrate the soil

191 according to (Iwata et al. 2008) and a surface pool of water is formed. The surface pool is subject

192 to freezing and thawing, and thus requires two state variables to represent the different phases:

193 liquid (water) and solid (ice) soil surface water. The rate of snow melt is calculated using a

194 degree–day temperature index K (mm °C$^{-1}$ day$^{-1}$), which is described by a sinusoidal curve with

195 a minimum in mid-winter and a maximum in mid-summer to incorporate the seasonal variation

196 in incoming radiation that influences snow-melt in addition to temperature (Thorsen et al. 2010).

197

198 The central organs of overwintering grass plants that determine sward survival are the apices of

199 the tillers. The apices of the overwintering (non-elongated) tillers are placed close to the soil

200 surface during winter, and thus sensitive to the micro-climatic conditions in this environment. In

201 BASGRA, the temperature at the soil surface is calculated as a function of the atmospheric

202 temperature, snow depth and soil frost depth. In the absence of snow or ice, the soil surface

203 temperature equals that of the atmosphere. The soil surface temperature below a cold insulating

204 snow cover is expressed as a function of snow cover depth, whereas the impact of soil frost

205 depth on soil surface temperature is described by more complex functions (Thorsen et al. 2010).

206

207 Effect of soil water on plant processes is mediated by the transpiration realisation factor

208 TRANRF (Höglind et al. 2001). This intermediate variable is calculated as a function of soil

209 water content, soil water retention characteristics, and plant transpirational demand. TRANRF

210 has a value of one when soil water content is at field capacity. It starts to fall when water

211 decreases below a critical level between field capacity and the wilting point, and it reaches zero

212 at the wilting point. Several processes are directly proportional to TRANRF, including

213 transpiration rate. Other processes that are affected are described in the following sections.

214 **2.3 Light interception, photosynthesis and allocation of carbon**

215 Light interception in BASGRA is modelled by Beer's law with a constant light extinction

216 coefficient operating on the leaf area index (LAI) (Höglind et al. 2001). However, in contrast to

217 LINGRA, the effect of snow cover on the availability of light is also taken into account. Thus,

218    when the ground is snow covered, a constant light extinction coefficient (KSNOW) for snow

219    operates in BASGRA, reducing the amount of light received by the plant canopy.

220    The rate of photosynthesis is modelled as the product of intercepted radiation and photosynthetic

221    light-use efficiency (LUEMXQ), which is a function of $CO_2$, temperature, light intensity and

222    Rubisco concentration of upper leaves (Rodriguez et al. 1999, Höglind et al. 2001). LUEMXQ

223    accounts for carbon lost to maintenance respiration, but not growth respiration. So the calculated

224    photosynthesis rate is gross photosynthesis minus maintenance respiration. LUEMXQ starts

225    decreasing linearly when temperature drops below one degree Celsius until it becomes zero at

226    minus four degrees according to observations made by Höglind et al. (2011). The latter is an

227    important improvement compared to LINGRA which overestimated photosynthesis at low

228    temperature (ibid.). Photosynthesis is also sensitive to drought and decreases with TRANRF.

229    BASGRA operates with five sinks: the processes of cold hardening, replenishment of the

230    reserves pool, leaf growth, stem growth, and root growth. Sink strengths are defined as the rate

231    at which these processes would proceed with no source limitation. The hardening process has top

232    priority, so its demand is met in full if source strength is large enough, irrespective of the four

233    other sinks. Root growth has lowest priority and depends on carbon unused by other sinks. The

234    strength priority between reserves on the one hand, and leaves and stems on the other hand

235    changes with day length. When day lengths are shorter than a cultivar-specific threshold,

236    reserves have higher priority than stems and leaves, with the opposite during the rest of the year.

237    Leaves and stems have equal priority so they receive carbon according to their sink strengths.

238    For comparison, in LINGRA leaves have top priority irrespective of season.

239    The sink strength associated with the growth of leaves is calculated as potential leaf area growth

240    (largely determined by temperature, but see also below) divided by specific leaf area (SLA). The

241    SLA of new leaf growth decreases linearly with reserve content. The sink strength associated

242    with the stem growth of elongating tillers decreases linearly with their biomass. The sink

243    strength related to growth of leaves and stems is also drought sensitive, decreasing linearly with

244    TRANRF. All these sink strength calculations are done in the same way as in LINGRA (Van

245    Oijen et al. 2005a). The sink strength associated with cold hardening, which is unique feature of

246    BASGRA, is expressed through the parameter KRESPHARD (g C $g^{-1}$ C $°C^{-1}$) which is defined

247    as the amount of C reserves needed to decrease the frost tolerance temperature (LT50, see

248 below) per gram of foliage by one degree Celsius. The C reserves pool is defined as the carbon

249 fraction of the water soluble carbohydrates in the plant.

## 2.4 Leaf area development

251 BASGRA distinguishes two leaf categories; leaves on vegetative and generative tillers (Höglind

252 et al. 2001). Leaf appearance rate depends on temperature, at a constant phyllochron, but slows

253 down under drought, short day length, and when the sward becomes dominated by generative

254 tillers at an advanced phenological stage. Potential growth rate of leaf area is proportional to the

255 product of the tiller density, the number of elongating leaves per tiller, a constant leaf width and

256 a temperature-dependent leaf elongation rate. All four factors in that product differ between

257 vegetative and generative tillers, so the calculation is done separately for the two categories and

258 then summed to give the potential growth of the total leaf area on all tillers. Leaf elongation rates

259 increase linearly with temperature, based on relationships determined by Peacock (1976) and

260 observations at Saerheim in south-western Norway (Höglind et al. 2005). The effect of day

261 length on leaf elongation is governed by the intermediate variable DAYLGE, with short days

262 restricting leaf elongation equally on both tiller categories. The sink strength related to growth of

263 leaves and stems is also drought sensitive, decreasing linearly with TRANRF.

264 BASGRA contains one state variable, which represents the phenological stage of the elongating,

265 generative tillers: PHEN. The value of PHEN increases at a rate that depends on temperature and

266 day length (Höglind et al. 2013). PHEN is reset to zero after each cut. Advancing PHEN stage

267 leads to reductions in leaf appearance rate (RLEAF) and in the number of elongating leaves for

268 this tiller category to account for the terminal growth behaviour of the generative tiller where

269 leaf elongation stops after the flag leaf has developed fully (Höglind et al, 2005). In contrast to

270 the original LINGRA model, leaf appearance in BASGRA is insensitive to the content of C

271 reserves, based on a previous study (Van Oijen et al. 2005a).

## 2.5 Tillering

273 BASGRA distinguishes three tiller categories: (1) vegetative tillers, (2) non-elongating

274 generative tillers, and (3) elongating generative tillers. The non-elongating generative tiller

275 category, which is new compared to the forerunner LINGRA, was added to make full-year

276 simulations possible for genotypes that have dual requirement for generative development: first a

277 requirement of low temperatures (vernalization) and then a requirement for long days (Heide,

278  1994). In BASGRA, vegetative tillers are formed at a rate that is proportional to leaf appearance
279  rate, but site-filling (proportion of potential tiller sites that produce tillers) is reduced when LAI
280  is high or C reserve content is low. This is new compared to LINGRA, where site filling is only
281  linked to LAI (van Oijen et al. 2005a). Vegetative tillers then move to the generative tiller
282  category at a rate that has a temperature optimum and a day-length dependency with fewer
283  generative tillers being formed at short day lengths. The day length dependent fraction of
284  vegetative tillers that moves to the generative tiller category (DAYLGE) is calculated as follows:

285    $$DAYLGE = (DAYL_t - DAYLB) / (DLMXGE - DAYLB); \quad 0 \leq DAYLGE \leq 1 \tag{1}$$

286  where $DAYL_t$ (d d$^{-1}$) is the fractional day length on day t, DAYLB (d d$^{-1}$) is the minimum day
287  length for vegetative tillers becoming generative, DLMXGE (d d$^{-1}$) is the minimum day length
288  for maximum generative tillering. The intermediate variable DAYLGE is also used for
289  calculating other day length dependent processes as described in other parts of the text.

290  Generative tillers move from the non-elongating to the elongating tillers category at a constant
291  daily rate as long as the day length is above the minimum day length required for this process
292  (Höglind et al. 2001). For Scandinavian timothy cultivars, this day length typically varies
293  between 14 and 18 h (Heide 1982). For genotypes with a vernalization requirement, this
294  transition from vegetative to non-elongating generative tillers only occurs after the vernalization
295  requirement has been fulfilled. In the current model version, the vernalization requirement is
296  simulated in a simplistic way using a threshold temperature. As soon as the temperature falls
297  below the threshold value, the vernalization requirement is considered fulfilled and vegetative
298  tillers start moving to the non-elongating generative tiller category. For genotypes without
299  vernalization requirement, the vernalization requirement in the model can be "bypassed" by
300  using a very high threshold temperature, e.g. 20 °C, allowing for generative tillers to be formed
301  already in the summer of the establishment year. Conversely, for cultivars with a vernalization
302  requirement, the formation of generative tillers may be inhibited until the winter in the
303  establishment year by using a low threshold, e.g. 0 °C. In timothy, many cultivars, including
304  Grindstad do not need to undergo vernalization to produce generative tillers. This is in contrast
305  to perennial ryegrass and many other grass species where most cultivars require vernalization to
306  initiate generative tillers.

307  **2.6 Senescence of leaves and tillers**

308    In BASGRA, the senescence rate of leaves and non-elongating vegetative and generative tillers

309    increases with LAI. Leaves, but not tillers, also die faster at higher soil surface temperatures.

310    Two other drivers of foliage death, frost and anaerobic conditions, are described in section 2.7.

311    The different processes leading to senescence are non-additive, i.e. the total senescence rate is

312    determined by the process for which the highest potential senescence rate is calculated on a

313    given day. The model does not simulate senescence of elongating tillers or roots. However,

314    cutting removes all elongating tillers, leaving a biomass fraction called stubble. This stubble dies

315    at constant relative rate during the first 1-2 weeks after cutting, allowing for remobilization of

316    the carbon reserves in the stubble and its reallocation to regrowing plant parts.

## 317    2.7 Cold hardening and impact of frost and ice encasement

318    Sensitivity to frost is measured by the state variable LT50, the "Lethal Temperature 50%", which

319    is the temperature that would kill half the leaves and non-elongating tillers if the sward was

320    subjected to a standardized freezing test (Höglind et al. 2010). The process whereby plants

321    reduce LT50, i.e. increase their level of frost tolerance, is called hardening. Dehardening

322    describes the loss of freezing tolerance due to triggering conditions, whereas rehardening

323    describes the regaining of freezing tolerance after a period of dehardening conditions (Kalberer

324    et al. 2006). The most important trigger of dehardening under field is mild weather conditions.

325    However, plants may also deharden in response to other stress events like anoxia (Höglind et al.

326    2010). In BASGRA, dehardening is sensitive to temperature but not to anoxia.

327    BASGRA simulates LT50 by estimating rates of hardening (RATEH) and dehardening

328    RATED). RATEH and RATED are simulated as dependent on the temperature at the soil surface

329    as in Thorsen and Höglind (2010). In short, hardening proceeds are fastest when LT50 is high

330    and temperatures low, and the opposite applies to dehardening.  A function which describes the

331    relationship between RATEH and the content of C reserves was introduced in BASGRA

332    according to observations (Hanslin and Höglind, 2009). RATEH is treated as a potential

333    hardening rate that can only be fully realized when the content of C reserves (CRES) is above a

334    threshold value, below which RATEH is linearly reduced. Hardening is hampered when

335    carbohydrate reserves drop below 20% of biomass, decreasing linearly to zero when reserves

336    become fully depleted. This compares to observed reserve levels in early winter (December-

337    January) of 13 % to 28 % of biomass for timothy cultivar Grindstad grown in Norway. The

338    estimated LT50 value is then used to calculate a relative death rate due to low temperatures in

339 the field. The fraction of leaves and tillers that survive for one day (RSRDAY) at the soil surface
340 temperature Tsurf is calculated using a truncated logistic curve:

341

342 $$RSRDAY = max\{ 0.5, 1 / [1 + exp(Tsurf-LT50_t)] \} \qquad (2)$$

343

344 where $LT50_t$ is the simulated LT50-value at time step *t*. The fraction of leaves and tillers that die
345 during one day due to frost, i.e. the relative death rate due to frost (RDRFROST) is thus

346

347 $$RDRFROST = 1 - RSRDAY \qquad (3)$$

348

349 When a surface ice layer is simulated, it is assumed that the plants are encapsulated in ice. As a
350 result, anaerobic conditions are created with the accumulation of by-products from anaerobic
351 respiration to toxic levels (Andrews, 1996). This phenomenon, often referred to as ice-
352 encasement, is a major cause of winter kill in perennial grasslands in regions with cold winters
353 like Northern Eurasia and Canada (Gudleifsson and Larsen, 1993). We estimate the number of
354 days with anaerobic conditions (TANAER) as the accumulated number of days with continuous
355 ice cover, and the number of ice-encapsulation days required to kill 50% of the leaves and tillers
356 is termed LD50. The LD50-value was related to the LT50-value based on observations for two
357 timothy cultivars (Grindstad and Engmo) (Höglind et al. 2010) using linear regression:

358

359 $$LD50 = LDT50A + LDT50B * LT50 \qquad (4)$$

360

361 Using the estimated LD50 value from Eq (4), the relative death rate due to the number of days of
362 ice encasement is derived as minus the normalized derivative of the curve for the fraction of
363 surviving plants: Relative death rate = - (d fSurv / dt) / fSurv. By describing the survival curve as
364 a logistic function of the number of ice-days (TANAER) with the inflection point LD50
365 calculated from Eq (4), the relative death rate due to ice encasement (RDRTOX) is estimated as:

366

367 $$RDRTOX = KRDRANAER / (1 + exp[-KRDRANAER (TANAER – LD50)]) \qquad (5)$$

368 where KRDRANAER ($d^{-1}$)  is the maximum relative death rate due to anaerobic conditions.

369 **2.8 Impact of cutting**

370 Most plant processes are interrupted during days when a cutting takes place. In BASGRA, the
371 cutting removes all elongating tillers, but no non-elongating tillers. All leaf area associated with
372 elongating tillers, and all leaf area associated with non-elongating tillers above a threshold is
373 removed by the cutting, as is the associated biomass and carbon reserves. A fixed fraction of the
374 stem biomass becomes stubble, and the stubble dies in a relatively short time allowing for
375 remobilisation of carbon reserves as described in section on senescence (2.6).

# 3 Model parameterisation

377 BASGRA was parameterized by means of Bayesian calibration as described by Van Oijen and
378 Höglind (2016). Here, we give a brief overview of the calibration procedure together with
379 additional results to those presented by Van Oijen and Höglind with special focus on simulated
380 results and observations for the winter season and the transitions between summer and winter.

## 3.1. Data

382 A dataset consisting of observations of the timothy cultivar Grindstad from experiments carried
383 out on five different locations in Norway was used to calibrate the model (Table 1). Short
384 descriptions of the different experiments are given below. Details on Exp. 1 can be found in
385 Höglind et al. (2006), on Exp. 2 in Höglind et al. (2010) and on Exp. 4 in Höglind et al. (2005).
386 Exp. 3 contains previously unpublished material (Sunde, 1996).

387 *Table 1. Sites with timothy experiments from which data were collected for calibration of the*
388 *BASGRA model, and for which simulations were performed in the example of application.*

| Location | Experiments | Latitude | Longitude | Elevation (m) | Climatic means, 1995-2012 | |
|---|---|---|---|---|---|---|
| | | | | | Temperature [1] (°C) | Precipitation (mm y$^{-1}$) |
| Apelsvoll | 3 | 60°70' N | 10°87' E | 255 | 4.8 (-6,6) | 679 |
| Fureneset | 1 | 61°29' N | 5°04' E | 12 | 7.7 (1.9) | 2280 |
| Holt | 1, 2 | 69°65' N | 18°90' E | 12 | 3.8 (-3.1) | 966 |
| Kvithamar | 1, 2 | 63°49' N | 10°88' E | 28 | 6.0 (-2.8) | 1007 |
| Særheim | 1, 2, 4 | 58°47' N | 5°41' E | 83 | 7.8 (1.0) | 1430 |

389 [1] Numbers without brackets show the mean annual temperature; numbers within brackets show the mean
390 temperature for the winter months December to February.
391

392 Exp. 1 was carried out at three locations: Fureneset, Holt, and Særheim (Table 1). The swards

393 were established in May (Fureneset, Særheim) or June 2005 (Holt). Shoot dry weight, leaf area

394 index (LAI), specific leaf area (SLA), tiller density, content of water soluble carbohydrates

395 (WSC), and frost tolerance (LT50) were determined on five occasions from November 2005 to

396 March 2006 at all three locations. In addition, tiller density and DM yield (total dry weight of

397 herbage above a stubble height of 5 cm) was determined in June 2006.

398

399 Exp. 2 was carried out at three locations: Holt, Kvithamar and Særheim (Table 1). The swards

400 were established in June 2005. From November 2006 to March 2007, on three occasions per

401 location, shoot biomass, tiller density, WSC, and LT50 were determined. In addition, tiller

402 density was determined at Særheim in June 2007. The swards were cut once (Holt) or twice in

403 the growing season 2006, and twice (Holt) or three times in the growing season 2007, and the

404 DM yield from each cut above a stubble of 5 cm was measured.

405

406 Exp. 3 was carried out at Apelsvoll (Table 1) in a sward established in May 1990. Sampling to

407 determine WSC and LT50 was carried out on 13 occasions between August 1990 and April

408 1991.

409

410 Exp. 4 was carried out at Særheim (Table 1). There were two fields. The first field was

411 established in 1999, with measurements taken in 2000. The other field was established in 2000,

412 with measurements taken in 2001 and 2002. Two cutting regimes were compared in each field.

413 From April to August each year, with sampling intervals of 7-14 days, shoot biomass, LAI, SLA,

414 tiller density, WSC, leaf appearance rate, number of elongating leaves per tiller, and leaf

415 elongation rate per actively growing leaf were determined.

416

417 All experimental locations were equipped with automatic weather stations, located within 500 m

418 from the experimental field. For the calibration of the model, daily weather data for the

419 individual sites, together with descriptions of the soils, were downloaded from the weather

420 database of Norwegian Institute for Agricultural and Environmental Research (present name

421 Norwegian Institute of Bioeconomy Research -NIBIO).

422

423 **3.2 Bayesian calibration**

424

425 Bayesian calibration of BASGRA consisted of three steps (Van Oijen et al. 2005b, 2013): (1)

426 defining the prior distribution for the model's parameters, (2) defining the likelihood function for

427 the model's parameters, (3) sampling from the 'posterior distribution' given by the normalised

428 product of prior and likelihood. The posterior distribution expresses how the data have reduced

429 our uncertainty about parameter values. Prior parameter ranges for individual parameters were

430 derived from earlier literature studies (Höglind et al. 2001; Van Oijen et al. 2005a; Thorsen et al.

431 2010) where available, whereas wide ranges of plausible values were assumed otherwise. All

432 plant parameters were treated as site-independent, whereas soil parameters were considered site-

433 specific.

434 The likelihood function quantified the probability, for any given parameter vector, of the

435 mismatch between the data and the model outputs induced by the parameter vector. The

436 measurement error terms in the likelihood function followed the conventional assumption of

437 independent Gaussians with variances that varied between variables and observations. The

438 sample from the posterior distribution was generated by means of Markov chain Monte Carlo

439 (MCMC) methods using the Metropolis algorithm (Metropolis et al. 1953; Van Oijen et al.

440 2005b). Chain length was 300,000 to ensure convergence for all parameters.

441 To quantify the mismatch between the data and the outputs from the calibrated model, we used

442 the Normalised Root Mean Square Error (NRMSE), which is the square root of the mean

443 squared difference between observations and outputs, divided by the mean of the observations.

444 The extent to which model output accounted for variation in the data was also quantified by

445 means of the square of Pearson's correlation coefficient ($r^2$).

## 3.3 Calibration results

447 The Bayesian calibration was carried out using data from five different sites on a total of ten

448 different variables. Table 2 and 3 gives an overview of the behaviour of BASGRA for biomass,

449 yield, C reserves, LAI, SLA, tiller density and LT50 when run with the MAP (*maximum a-*

450 *posteriori*) parameter estimates from the Bayesian calibration. Using this parameter vector,

451 nearly all variables were simulated to an overall NRMSE less than 0.5 (Table 2). In a third of the

452 site x experiment combinations, NRMSE was below 0.3 (Table 3), and median NMRSE for the

453 combined dataset was below 0.4 for nearly all variables (Table 2). For leaf appearance rate, leaf

454 elongation rate, and elongating leaf density, respectively, NMRSE was 0.46, 0.53 and 0.70.

455

456 *Table 2. Normalised Root Mean Square Errors (NRMSE) and squared Pearson's correlation*
457 *coefficients ($r^2$) for the mismatch between simulations and the data when running BASGRA with*
458 *the maximum a posteriori (MAP) parameter estimates from the Bayesian calibration.*

| | Mean of data for all sites | Mean of simulations for all sites | Mean NRMSE for the total dataset | Median NRMSE for the total dataset | $r^2$ for the total dataset |
|---|---|---|---|---|---|
| Aboveground DM (g m$^{-2}$) | 309 | 282 | 0.39 | 0.37 | 0.93 |
| Reserves (g g-1) | 0.15 | 0.12 | 0.40 | 0.37 | 0.38 |
| DM yield (g m$^{-2}$) | 312 | 409 | 0.51 | 0.38 | 0.64 |
| LAI (m$^{-2}$ m$^{-2}$) | 3.3 | 3.1 | 0.44 | 0.46 | 0.81 |
| SLA (m$^{-2}$ g$^{-1}$) | 0.026 | 0.028 | 0.27 | 0.35 | 0.27 |
| Tiller density (m$^{-2}$) | 2542 | 2307 | 0.41 | 0.34 | 0.48 |
| LT50 (°C) | -14.9 | -15.2 | 0.23 | 0.19 | 0.75 |

459 *Table 3. NRMSE for the mismatch between simulations and data when running BASGRA with the MAP*
460 *parameter estimates from the Bayesian calibration split on individual experimental sites and experiments.*
461 *Abbreviations in column headers refer to site names and experiment numbers listed in Table 1 (ex. Ap1 =*
462 *Apelsvoll Exp. 1). Sa4 denotes the combined data from the two experimental seasons and two harvest*
463 *regimes of Exp. 4.*

| | | Ap3 | Fu1 | Ho1 | Ho2 | Kv2 | Sa1 | Sa2 | Sa4 |
|---|---|---|---|---|---|---|---|---|---|
| Biomass (g m$^{-2}$) | Mean of data | - | 162 | 27 | 24 | 92 | 24 | 52 | 384 |
| | NRMSE | - | 0.23 | 1.14 | 0.59 | 0.19 | 1.21 | 0.81 | 0.36 |
| Reserves (g g$^{-1}$) | Mean of data | 0.20 | 0.12 | 0.16 | 0.18 | 0.15 | 0.17 | 0.20 | 0.13 |
| | NRMSE | 0.43 | 0.13 | 0.54 | 0.44 | 0.71 | 0.26 | 0.37 | 0.37 |
| Yield (g m$^{-2}$) | Mean of data | - | 346 | - | 638 | 297 | - | 278 | - |
| | NRMSE | - | 0.34 | - | 0.45 | 0.35 | - | 0.41 | - |
| LAI (m$^2$ m$^{-2}$) | Mean of data | - | 1.3 | 0.2 | - | - | 0.3 | - | 3.8 |
| | NRMSE | - | 0.27 | 0.65 | - | - | 2.67 | - | 0.41 |
| SLA (m$^2$ g$^{-1}$) | Mean of data | - | 0.029 | 0.033 | - | - | 0.020 | - | 0.026 |
| | NRMSE | - | 0.31 | 0.32 | - | - | 0.23 | - | 0.26 |
| Tiller density (m$^{-2}$) | Mean of data | - | 1866 | 694 | 1282 | 2987 | 1685 | 2385 | 2755 |
| | NRMSE | - | 0.32 | 0.34 | 1.06 | 0.18 | 0.22 | 0.52 | 0.40 |
| LT50 (°C) | Mean of data | -12.8 | -12.4 | -14.9 | -16.9 | -20.0 | -17.7 | -14.7 | - |
| | NRMSE | 0.33 | 0.19 | 0.12 | 0.10 | 0.18 | 0.23 | 0.17 | - |

464

465



466

467
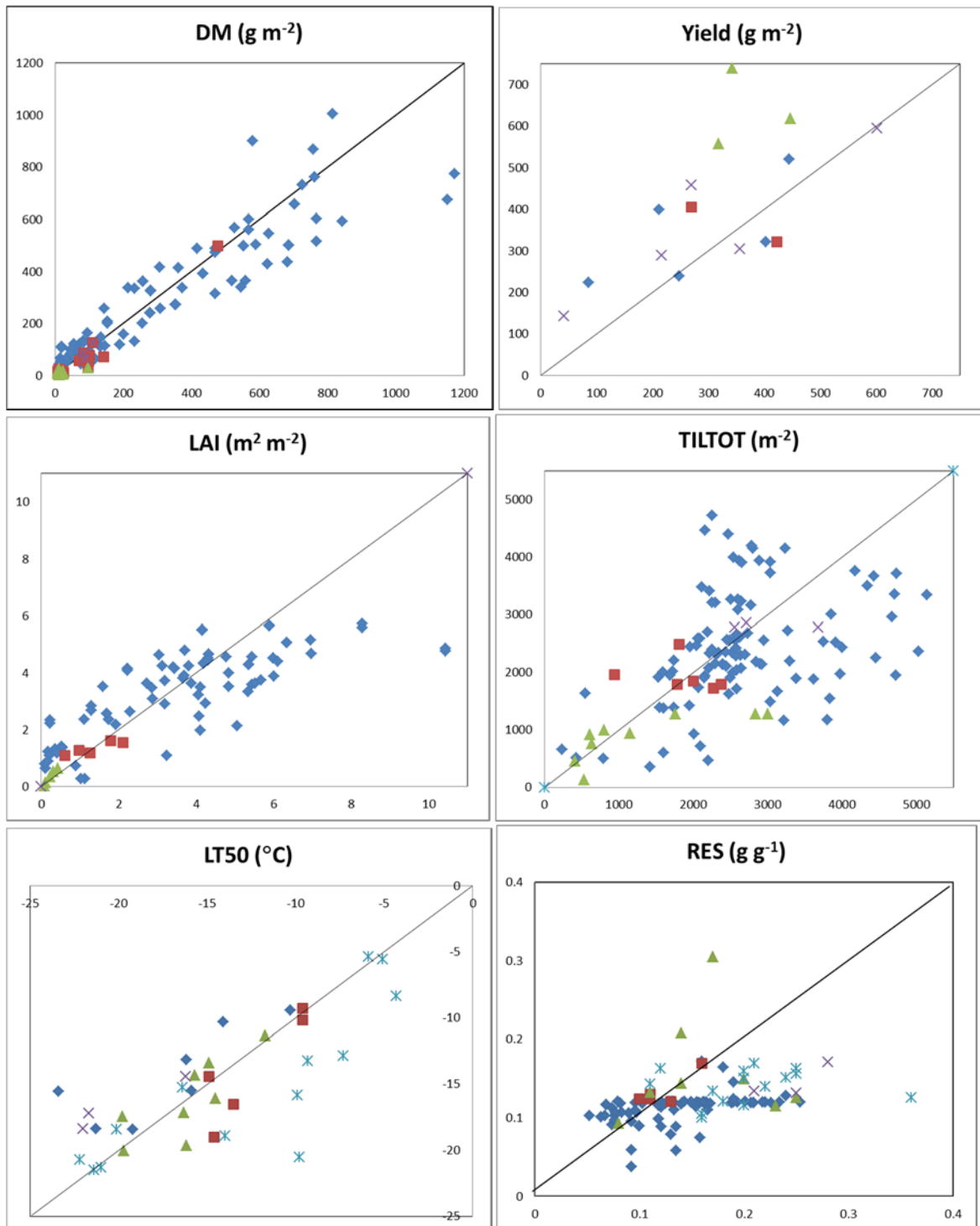
*Figure 1. Collective scatterplots of measured (x-axis) versus simulated (y-axis) dry matter (DM), yield*

*(Yield), leaf area index (LAI), tiller density (TILTOT), frost tolerance (LT50) and reserve content (RES)*

*for timothy when running BASGRA with the MAP parameter estimates from the Bayesian calibration.*

*Blue diamonds: Særheim; blue x-signs: Fureneset; light blue stars: Apelsvoll; green triangles: Holt; red*

*squares: Kvithamar.*

473



474
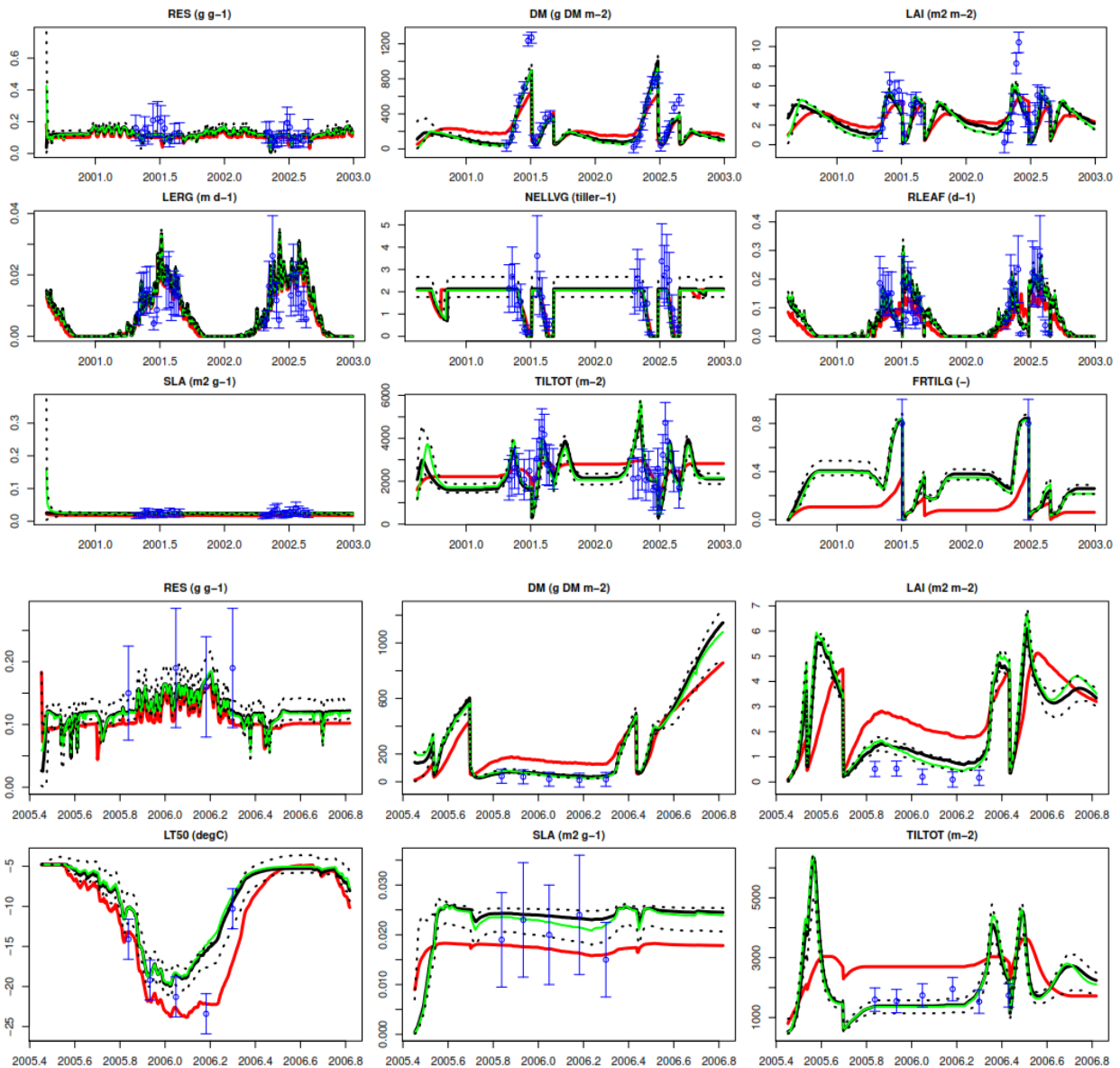
*Figure 2. Results of Bayesian calibration, showing prior and posterior time series with a) the observations of the late cutting regime of Exp 4 carried out at Særheim in 2001-2002 (the nine uppermost graphs; this experiment included summer observations only), and b) all the observations of Exp 3 carried out at Særheim in 2005-2006 (lowermost six graphs; this experiment included winter observations only). Blue: observations ± standard deviation (SD). Red: model outputs for the mode of the prior distribution. Black: model outputs for the posterior mode ± SD: Green: model outputs for the parameter vector with highest likelihood. RES: reserve content, DM: dry matter, LAI: leaf area index, LERG: leaf elongation rate, NELLVG: number of elongating leaves per tiller, RLEAF: leaf appearance rate, SLA: specific leaf area, TILTOT: tiller density, FRTILG: fraction of tillers that is generative, LT50: frost tolerance.*

484    Based on NRMSE, the model performed best for the variables LT50 followed by SLA and

485    biomass, whereas in terms of $r^2$ it performed best for biomass followed by LAI and LT50 (Table

486  2). The scatterplots of measured and simulated values presented in Fig. 1 indicate a tendency to
487  underestimate high biomass and LAI values. The simulated biomass yield was higher than the
488  observed biomass yield for most of the observations. The scatterplots for tiller density and
489  reserves show more extreme deviations between simulations and observations compared with
490  those for biomass, yield, LAI and LT50.

491  Fig. 2 shows an example of the impact of the Bayesian calibration on the model behaviour for
492  two experiments at the most data rich-site, Særheim. The temporal dynamics of the ten variables
493  were in general well captured. This applies both for the summer and winter data. Corresponding
494  graphs for the remaining experiments are presented as Supplementary material.

## 4 Model application: time courses of growth and underlying processes at two contrasting sites in Norway

497  We now show an example of application of BASGRA for the simulation of multiple consecutive
498  years of timothy grass growth and underlying processes. This section is intended to highlight the
499  capacity of the model to study overwintering processes and their linkages with preceding and
500  following growing seasons. Simulations were performed for two sites in Norway, Holt and
501  Særheim (Table 1). The northern location Holt is characterized by relatively harsh, unstable
502  winter conditions, whereas Særheim generally has milder winter conditions (Table 1). At each
503  site, simulations were performed for six three-year long grass rotations for the period 1995 to
504  2012. Two harvests per year were simulated, with harvest dates adjusted to local climate
505  conditions (Höglind et al. 2013). BASGRA was re-initialized in the beginning of each growth
506  cycle using the MAP values from the Bayesian calibration.

507  The 3-year cycles with the highest and lowest total dry matter yield for each site are shown in
508  Fig. 3. According to agricultural insurance pay-out statistics, perennial grasslands survive most
509  winters well in the region where Særheim is located (Rogaland county), whereas severe winter
510  injury occurs every three to four years in the region where Holt is located (Troms county;
511  Landbruksdirektoratet, https://www.slf.dep.no/no). The difference in winter conditions between
512  the locations is also reflected in the simulation results. At Holt the winter survival varied
513  considerable between years, and growth cycles. Notably a severe winter kill was simulated in the
514  first winter of the 1999-2001 growth cycle, resulting in very poor total yield. This contrasts to
515  Særheim, for which only minor differences in survival and yield between the growth cycles were

516     simulated. Further examination of the results reveal that anoxic conditions due to a long period

517     of ice encasement was the major cause of winter kill in the poor 3-year cycle at Holt. Figure 4a

518     shows that one single event of prolonged anoxia and virtually no frost stress was simulated

519     during the poor 3-year cycle at Holt. This contrast to the corresponding 3-year cycle at Særheim

520     where virtually no winter stress of any type was simulated (Fig. 4b) although some very light

521     frost stress is revealed if the graph is scaled up (not shown).
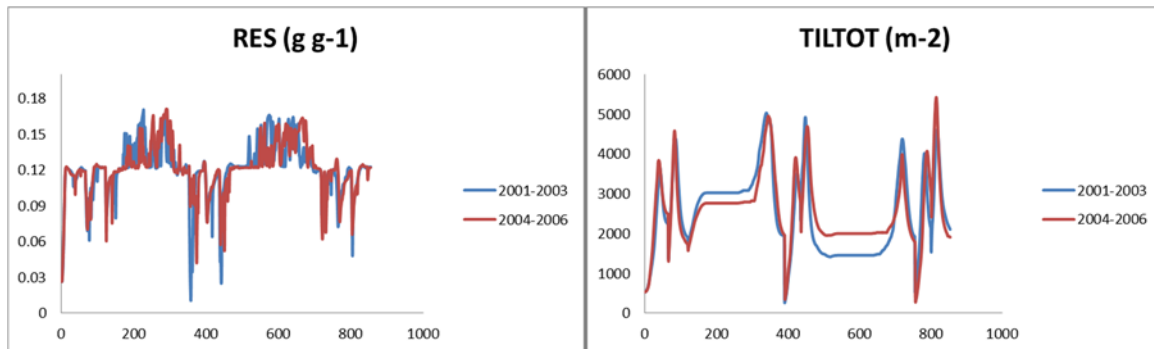


522
523
524
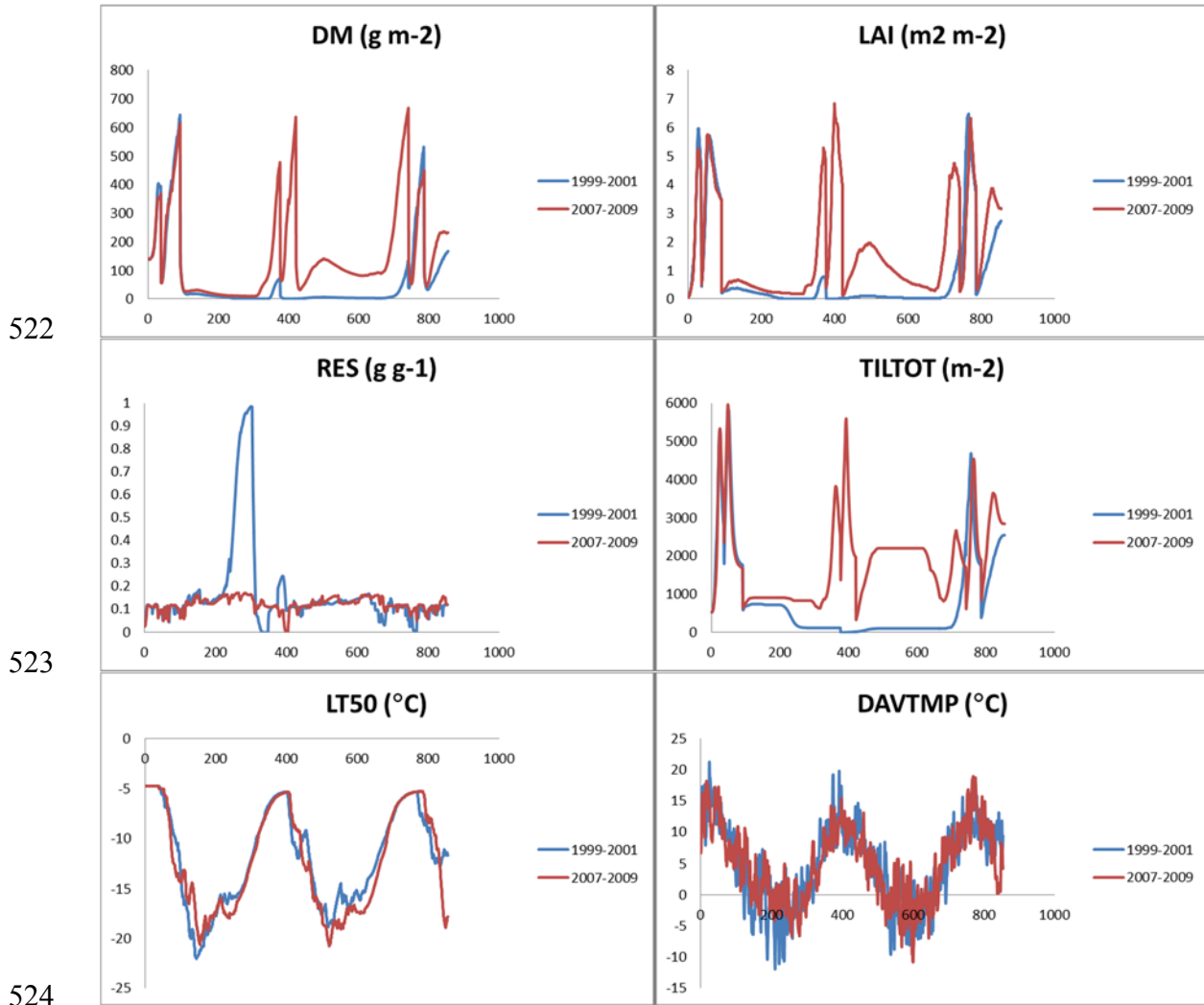
*Figure 3a. Simulation results for timothy grown at Holt in the 3-year cycle with the highest (2007-2009)*

*and lowest (1999-2001) total dry matter yield within the period 1995-2012. The x-axis shows the number*

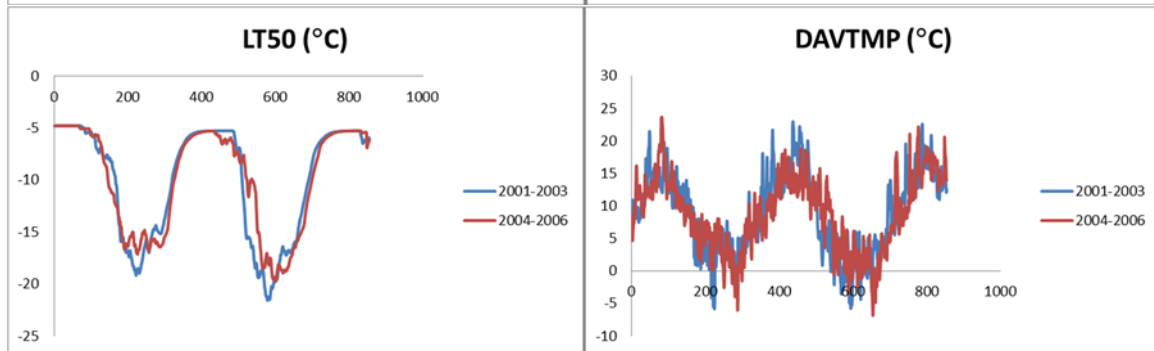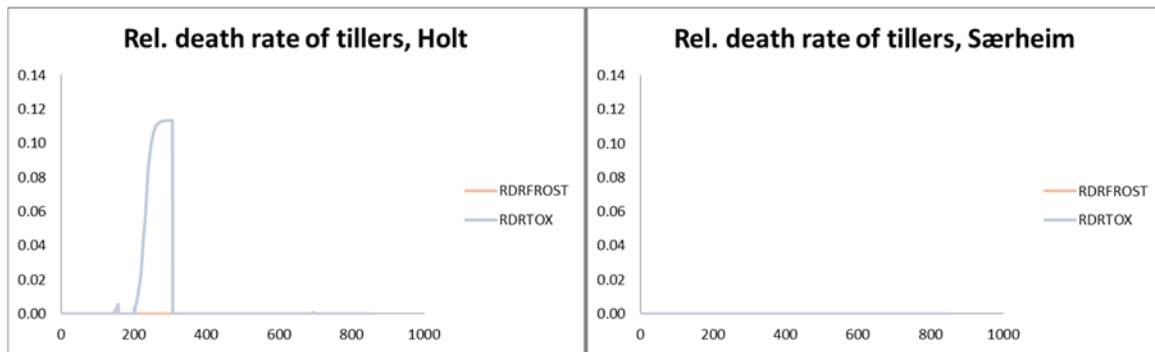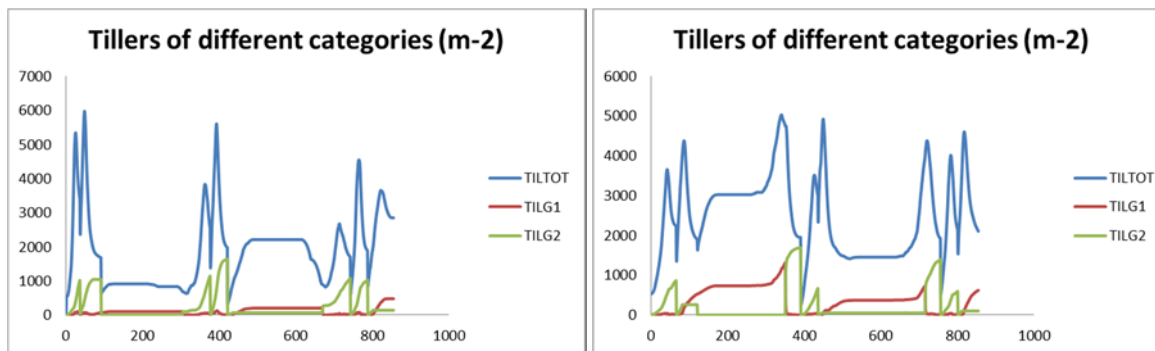*of days since the start of simulation at sward establihment (19 June).*

529

530

531
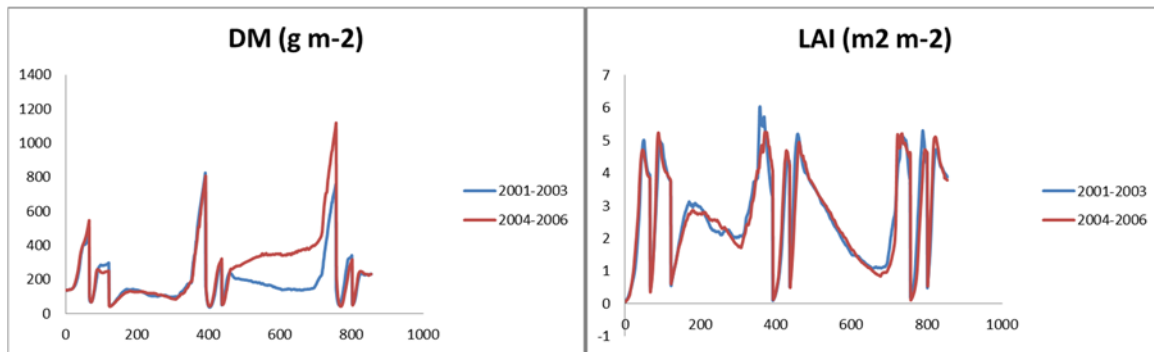
*Figure 3b. Simulation results for timothy grown at Særheim in the 3-year cycle with the highest (2004-*
*2006) and lowest (2001-2003) total dry matter yield within the period 1995-2012. The x-axis shows the*
*number of days since the start of simulation at sward establishment (20 May).*

A new feature of BASGRA compared with LINGRA is the additional tiller fraction representing
generative, non-elongating tillers. The contribution of the different tiller categorises to the total
tiller population and the relationship between them is exemplified in Fig. 5. At Holt, tillers
mainly overwinter in the vegetative stage and the transition from vegetative to non-elongating
generative tillers and further on to elongating tillers in spring is very quick. This contrasts to
Særheim where both vegetative and non-elongating tillers survive, and where the transition
between the non-elongating and elongating generative tillers starts earlier and takes more time,
reflecting the more gradual increase in temperature and day-length at the southern location, as
observed in controlled experiment with different temperature and day lengths (Heide 1982)

544

*Figure 4. Simulated relative death rates of tillers due to frost (RDRFROST) and ice encasement (RDRTOX) stress at Holt 1999-2001 (left) and Særheim 2001-2003 (right). The x-axis shows the number of days since the start of simulation at sward establishment (19 June and 20 May, respectively).*

545
546
547



548

*Figure 5. Simulated density of non-elongating( TILG1) and elongating (TILG2) generative tillers and total tillers (TILTOT) at Holt 2007-2009 (left) and Særheim  2004-2006 (right). The x-axis shows the number of days since the start of simulation at sward establishment (19 June and 20 May, respectively).*

549
550
551

552 Fig. 6 presents normalized time courses for the average middle year of the six 3-year cycles that
553 were simulated. These graphs illustrate the difference in growing conditions between the two
554 sites, such as the longer growth season at Særheim, with earlier accumulation of biomass, leaf
555 area development and tiller production and later cessation of these processes in autumn
556 compared with Holt. These differences in spring and autumn growth between the two sites can,
557 to a large extent, be explained by the differences in temperature and day-length conditions. Cold
558 hardening is also controlled by temperature, as expressed in the faster development of simulated
559 frost tolerance at the colder site compared with the warmer site Særheim. The faster simulated
560 loss of frost tolerance (dehardening) in spring at Holt may at first look surprising given the lower
561 mean winter temperature at this site. However, this site experienced repeated freeze/thaw events
562 that, according to the simulation, lead to ice encasement and loss of C reserves in several of the
563 winters, reducing the rehardening capacity of the sward more than at Særheim where C reserves

564     were better maintained, as also observed in experiments at the two sites (Höglind et al. 2006,

565     2010).

566



567

568
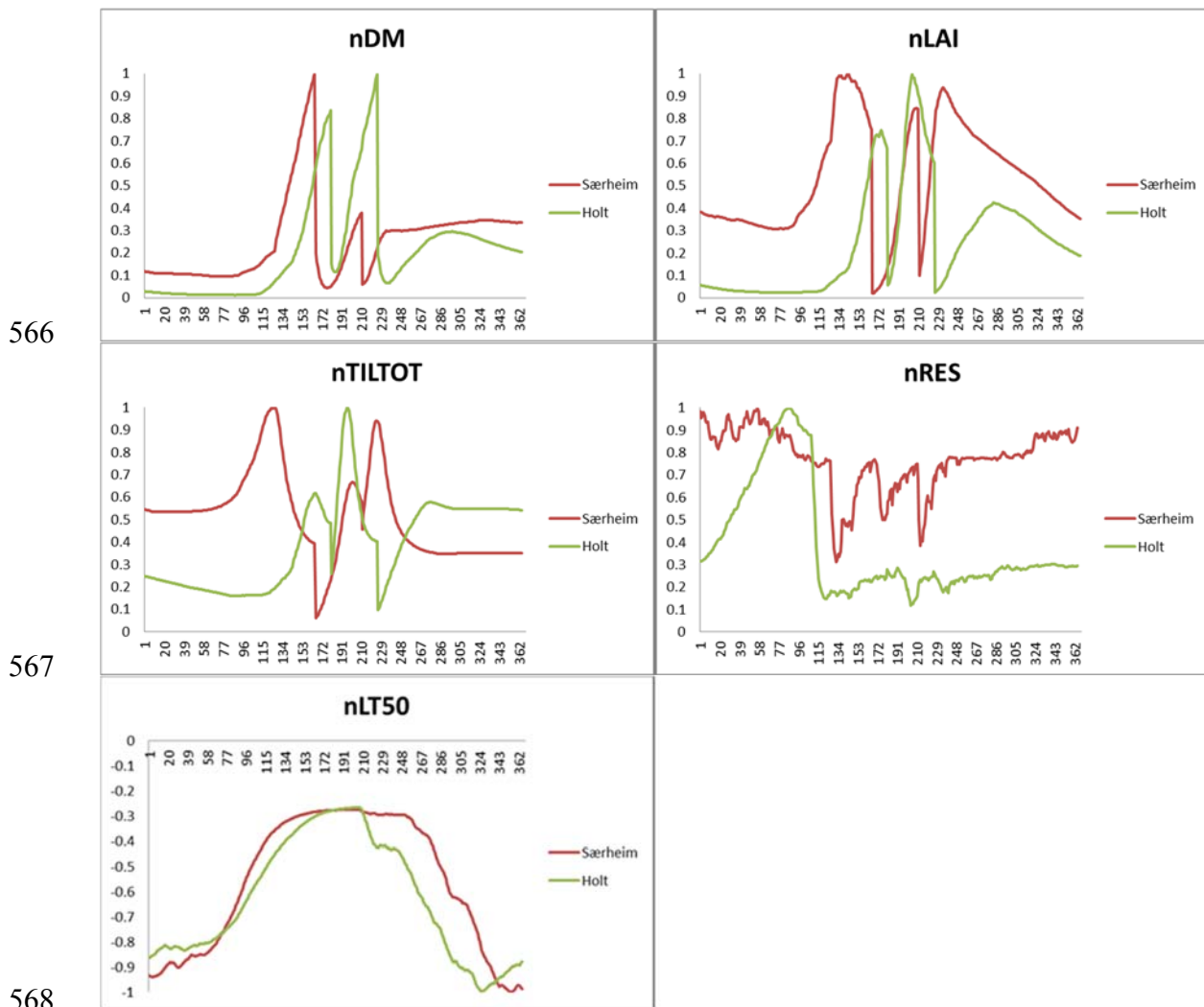
569     *Figure 6. Normalized dry matter (nDM), leaf area index (nLAI), tiller density (nTILTOT), reserve content*

570     *(nRES) and frost tolerance (nLT50) for the average second year of all the 3-year growth cycles that were*

571     *simulated for timothy at locations Særheim and Holt (1995-1997, 1998-2000, 2001-2003, 2004-2006,*

572     *2007-2009, 2010-2012). All variables are expressed relative to the maximum value across the six cycles.*

573     *The x-axis shows the day number of the year.*

574     # 5 Discussion and outlook

575     **5.1 Unique features of BASGRA**

576     The BASGRA model is unique in several ways. Most important, it is the first process-based

577     model for temperate grasslands that is able to simulate grass growth and survival for time series

578 of full, consecutive years taking into account the ability of the plant to cold acclimate, and the
579 effect of cold winter conditions on plant growth and survival. This was made possible by
580 incorporating algorithms representing plant processes and control mechanisms which are usually
581 not represented in grassland models. While any process-based model is a simplification of reality
582 as it only includes the driving variables and physiological mechanisms that are considered the
583 most important for the intended use of the model, it is important that it is based on current
584 ecophysiological and agronomical knowledge. In the following, we discuss some of the central
585 features of BASGRA in relation to current knowledge.

586 A novel important feature of BASGRA is the simulation of cold hardening as a function of
587 temperature (Gay and Eagles, 1991; Fowler et al.1999), availability of reserves (Hanslin and
588 Höglind, 2009), and time (Rapacz et al. 2014). For winter wheat, it has been shown that the
589 ability to reharden after a mild episode is closely linked to the development stage of the tillers,
590 with a reduction of the ability to reharden after the vernalization requirement has been fulfilled
591 (Mahfoozi et al. 2001). In BASGRA, the ability to reharden is linearly decreased with time
592 between mid-winter and spring. A more complex modelling approach including a link between
593 vernalization and rehardening capacity did not give better simulations than the simpler approach
594 used in the present model (Thorsen and Höglind, 2010). This fits well with recent observations
595 indicating that vernalization and rehardening ability may not be as closely linked in forage
596 grasses as in wheat (Seppänen et al. 2010; Rapacz et al. 2014). However, more research is
597 needed before conclusions can be drawn on how rehardening capacity should ideally be
598 modelled. There may be large but still unknown genetic variation in vernalization requirement
599 and links between vernalization and rehardening capacity between timothy cultivars.

600 Short day length may stimulate hardening further under low temperatures as long as there is
601 enough light for this energy demanding process (Rapacz et al. 2014). In BASGRA, we have
602 incorporated an indirect effect of day length on cold hardening via the dependency of cold
603 hardening on the content of carbohydrates, and the changed priority order for assimilates from
604 growth to carbohydrate storage at short day lengths. There is also a direct control of short day
605 length on leaf elongation in BASGRA, leading indirectly to a reduced demand of carbon for
606 growth at short day lenghts. The data presented in this paper suggest that this approach works
607 well. However, it should be noted that there are still many unresolved questions on how growth
608 cessation in forage grasses is controlled, with multiple interacting factors including day length,

609   temperature and genotype (Rapacz et al. 2014). When more knowledge becomes available, it

610   will be possible to develop BASGRA further with respect to these processes and their controls.

611   Ice encasement tolerance in BASGRA is calculated using a simple approach where it is linearly

612   related to frost tolerance, although these two tolerances do not share the same mechanisms

613   (Höglind et al. 2010). A simple approach is also used for calculating ice encasement related

614   mortality, where ice encasement exposure is purely a function of time. A more mechanistic

615   approach could include an estimation of the accumulation of toxic compounds from anaerobic

616   respiration in the plants (Bertrand et al. 2003) as a function of the availability of carbon reserves

617   in the plants, the respiration rate of the encapsulated plant and soil biota, the volume of the ice

618   encapsulated air space, and the rate of gas exchange with the surrounding atmosphere in case the

619   ice is not fully impermeable (Andrews, 1996).

620   **5.2 Calibration results**

621   For the calibration we used detailed data on the growth and development of timothy grass swards

622   and individual plants from five different locations in Norway, with up to five years of

623   observations per site from either the summer or winter season or a combination of both seasons.

624   The sites and years represent a wide range of climate and weather conditions as well as other

625   environmental conditions like day length (latitudes from 59° to 70° N) and soil types (sandy to

626   silty loams/clay loams). The total dataset included 11 variables, including biomass, LAI, tiller

627   density, WSC content and LT50, with up to eight variables per site. The results of the calibration

628   show that a single parameter vector, the MAP, suffices to simulate nearly all measured variables

629   to a NRMSE of less than 0.5. This is in the same order of magnitude as the coefficient of

630   variation of the data. For about a third of the site x experiment combinations, NRMSE was

631   below 0.3, and median NMRSE for the combined dataset was below 0.4 for most variables.

632   The dataset from Exp. 4 was also used in a previous study (Van Oijen et al. 2005a) where the

633   LINGRA model was evaluated. As LINGRA is the predecessor of BASGRA, it is interesting to

634   note that the NMRSE and $r^2$ values obtained here for BASGRA using the data from Exp. 4, are

635   at least as good as those obtained for LINGRA when only the summer season was taken into

636   account. For many variables including biomass, BASGRA gave slightly lower NMRSE and

637   higher $r^2$ values than LINGRA. This means that the changes introduced to turn the summer

638   model LINGRA into the full-year model BASGRA, are a step forward not only in allowing for

639 full-year simulations including winter processes, but also in simulating summer processes with
640 increased precision.

641 The plots of simulated versus observed data presented in Figures 2 confirm that biomass, an
642 output variable that is in many cases the one that is considered the most important, is simulated
643 with good accuracy. However, harvested yield is generally overestimated. However, as biomass
644 in general is satisfactorily simulated, this indicates that the harvested fraction of the aboveground
645 biomass is systematically overestimated rather than dissatisfactory simulation of biomass. LAI
646 and LT50 are also simulated with relatively good accuracy. Further, the temporal dynamics of
647 these variables, as well as of several other variables were captured in a satisfactory way by the
648 model, as evident from the time courses of simulated versus observed data presented in Figure 3
649 (Særheim x 2) and as Supplementary material (remaining experiments).

650 However, some variables, notably tiller density and reserve content are simulated with less
651 accuracy, calling for model improvements with respect to the underlying processes influencing
652 those variables. Such work would require more data, preferably from experiments with detailed
653 measurements carried out throughout full life-cycles of three to four years, including
654 observations in winter as well as summer on at least the 5-6 most central variables studied here.
655 Currently, we have no clear answer to how to improve BASGRA with respect to simulation of
656 tiller density and C reserves. The strong dependency of tillering on C reserves, and the mutual
657 dependency of C reserves on the regrowth of tillers with photosynthetic tissue after a cut or
658 stressful winter indicate that if the simulation of the processes governing one of these variables
659 could be improved, the simulation of the processes governing the other might also be improved.
660 Tiller density and C reserves are both sensitive to nitrogen availability (Höglind et al. 2001). The
661 experiments from which the data used to calibrate our model were obtained had all received
662 relatively high levels of nitrogen fertilizer, and we assumed non-nitrogen limiting growth
663 conditions for all experiments. However, it cannot be excluded that nitrogen limited growth
664 occurred occasionally in one or more of the experiment, for example in connection with dry soil
665 conditions, which would affect tillering and C reserves in ways not accounted for in the model.

666 Taken together, the results of the comparison of simulations and observations may suggest that
667 the BASGRA model is fairly robust, with an ability to simulate both the growth of the grass
668 sward and important underlying processes with acceptable accuracy for a wide range of
669 agroclimatic conditions without the need for site-specific parameterization, at least not for the
670 range of geoclimatic variation considered here which included a wide latitudinal range.

671 However, we need to test the robustness of the model further by comparing the behaviour of

672 BASGRA for sites in Norway with its behaviour for sites in other countries. Such work is

673 underway for sites in Canada and Finland (Korhonen et al. in prep.).

**5.3 Further validation**

675 Parts of the BASGRA model have been validated before. The LINGRA model, parameterized

676 for the same timothy cultivar as was used in the present study, i.e. Grindstad, was evaluated with

677 respect to simulation of timothy dry matter yields over a wide range of agroclimatic conditions

678 represented by seven locations in Iceland, Norway, Sweden and Finland (Persson et al. 2014).

679 The frost tolerance model, parameterized for the Norwegian timothy cultivar Engmo, was

680 validated with respect to simulation of LT50 using data from four Norwegian locations (Thorsen

681 and Höglind, 2010). Finally, the SnowFrostIce model was validated for simulation of snow, ice

682 cover and frost depth using independent observations from five Norwegian sites (Thorsen et al.

683 2010). A slightly modified version of SnowFrostIce was also validated with satisfactorily results

684 with respect to simulation of snow cover dynamics in Canada (Jégo et al. 2014).

685 We used all the detailed data on Grindstad timothy growth and development during summer and

686 winter seasons for the calibration that were available for this study, not leaving any independent

687 data for validation. This choice was made to get a more robust calibration than what a smaller

688 dataset would have made possible, the overall aim being to develop a model that would not need

689 site-specific calibration for plant parameters. However, even though the simulations with the

690 calibrated model described the calibration dataset with acceptable accuracy, a thorough

691 validation of BASGRA against independent data should be performed when such data become

692 available. There is specifically a need to validate the model for simulation of multiple

693 consecutive years with variable overwintering conditions.

694 A possible approach for validation of BASGRA with respect to simulation of winter survival and

695 subsequent growth under different climatic conditions would be to, as a starting point, use the

696 same dataset that was used in the validation of the LINGRA model for summer growth (Persson

697 et al. 2014). In the cited study, LINGRA was run for single summer seasons and locations using

698 a common set of standard initial values for biomass, tiller density and LAI representing typical

699 sward conditions in spring, with re-initialization of the model each spring. The model was

700 evaluated by comparing observed and simulated dry matter yields from two to three harvests per

701 year. To validate BASGRA, the model should not only be run for single growing seasons as in

702 the cited study, but also continuously from establishment throughout the lifetime of the sward

703 (generally three seasons) including winters. A rough test would be whether consecutive full-year

704 simulations will give lower mismatch between observed and simulated yields compared to re-

705 initializing the model each spring using standard initial values not accounting for possible

706 differences in winter survival between locations and years.

707 **5.4 Scope for application**

708 A full year grassland model like BASGRA that takes into account cold hardening and the effect

709 of winter conditions on plant growth and winter survival, can be applied in many types of

710 studies, addressing various types of questions. In a recent paper, we discuss the possibility to use

711 BASGRA for designing grass ideotypes for current climate conditions (Van Oijen and Höglind,

712 2016). This approach could also be applied to conditions of climate change. A number of climate

713 change impact studies have been carried out using grassland models focusing on summer growth

714 processes (Riedo et al. 1999; Höglind et al. 2013; Persson and Höglind, 2014; Jing et al. 2014).

715 A natural extension of these studies would be to include the effect of the expected climate

716 change on the winter survival of the grass sward and subsequent effects on yield.

717 BASGRA also has a great potential as a tool for tactical planning in relation to winter survival.

718 Forecasts of winter injury could for example help seed suppliers to make sure that enough seed

719 is available for reseeding in years with severe winter injury. In such years, seeds are commonly

720 imported from regions with less winter injury. The sooner the seed supplier can have the right

721 seed available in spring, the sooner the farmer can reseed, thus minimizing the non-productive

722 time and increasing the yield potential of the sward. The example application presented in

723 section 4 suggests that BASGRA may be suitable for such planning.

724 Finally, we note that BASGRA can be applied to other grassland species than timothy. This may

725 include species such as perennial ryegrass (*Lolium perenne* L.) that are sown at greater density

726 and have less winter tolerance and greater vernalization requirement than timothy. This would

727 require changes in model initialisation and calibration but no changes in model structure.

728 **5.5 Further development**

729 BASGRA takes into account the effects of frost, snow and ice conditions on grass growth,

730 development and winter survival. Frost and ice related winter injuries are especially common in

731  high-latitude regions with coastal types of climate conditions typically characterized by variable

732  snow conditions and relatively frequent episodes of freezing and thawing (Larsen, 1994). Such

733  conditions are for example common along large parts of the Norwegian coast, where some of the

734  most productive grasslands in this country are located. Frost and ice may also cause severe

735  winter injury in inland areas with more stable snow conditions, especially in atypical years with

736  less stable snow conditions. However, in inland regions, especially those which experience long

737  and stable snow cover, fungal diseases are often a more common cause of winter injury than

738  frost and ice encasement (Larsen, 1994).

739  Given the importance of fungal diseases for winter survival in certain agricultural regions, a

740  natural further development of BASGRA would be to include functions for simulating the

741  development of snow mould fungi on the plant, and the plants' response to snow mould

742  infection. The strong interaction that exists between host and parasite for disease development

743  and level of winter injury makes this a challenging task (Raspacz et al. 2014). However, the

744  ability of BASGRA to simulate frost tolerance and snow cover is a good starting point as: (1)

745  resistance to snow mould fungi and frost tolerance are often highly correlated (although frost

746  tolerance and disease resistance may have different mechanisms) (Tronsmo, 1984), and (2) snow

747  condition is an important factor controlling disease development (Matsumoto, 2009).

748  **5.6 Conclusions and outlook**

749  With BASGRA, we have taken an important step toward full-year simulations of timothy yield

750  that take into account the major winter stress factors contributing to yield variability in

751  Scandinavia and regions with similar conditions. The current version of BASGRA allows for

752  simulation of cold hardening and dehardening and the effect of cold temperatures, snow and ice

753  conditions on survival and yield. However, the effect of fungal diseases on winter survival is not

754  yet accounted for, which would be needed to fully capture winter stress related yield variability

755  in these regions. The comparison of simulations and observations for the 11 different variables in

756  the calibration dataset indicate that BASGRA is a reasonably robust model with which the

757  growth and important underlying processes in timothy swards can be simulated with acceptable

758  accuracy for a fairly wide range of agroclimatic conditions. However, the robustness of the

759  model needs to be tested further using independent data from different agroclimatic conditions

760  and grass management regimes. BASGRA can also be parameterized for other species, and we

761  are currently collecting calibration data for perennial ryegrass. Further work will include

762  improvement of the model with respect to simulation of tillers and C reserves, incorporation of

763     N-dependent growth functions, and validation against independent data for the conditions for

764     which it will be used.

## 6 Acknowledgments

## 7     References

775     Andrews, C.J., 1996. How do plants survive ice? Annals of Botany 78, 529-536.

776     Bélanger, G., Rochette, P. Castonguay, Y., Bootsma, A., Mongrain, D., Ryan, D.A.J., 2002.

777       Climate Change and Winter Survival of Perennial Forage Crops in Eastern Canada.

778       Agronomy Journal 94, 1120–1130.

779     Bertrand, A., Castonguay, Y., Nasdeau, P., Laberge, S., Rochette, P., Michaud, R., Bélanger, G.,

780       Benmoussa, M., 2001. Molecular and biochemical responses of perennial forage crops to

781       anoxia at low temperature. Plant, Cell and Environment 24, 1085–1093.

782     Bonesmo, H, Bélanger, G., 2002. Timothy yield and nutritive value by the CATIMO model: I.

783       Growth and nitrogen. Agronomy Journal 94, 337-345

784     Fowler, D., Limin, A., Ritchie, J., 1999. Low-temperature tolerance in cereals: model and

785       genetic interpretation. Crop Science 39, 626–633.

786     Gay, A.P., Eagles C.F., 1991. Quantitative analysis of cold hardening and dehardening in

787       Lolium, Annals of Botany 67: 339-345.

788     Gudleifsson, B.E., Larsen, A., 1993. Ice encasement as a component of winter kill in herbage

789       plants. In: Li P.H., Christerson, L. (eds), Advances in plant cold hardiness. London, UK: CRC

790       Press., pp. 239–249.

791 Hanslin, H., Höglind, M., 2009. Differences in winter-hardening between phenotypes of Lolium
792   perenne with contrasting water-soluble carbohydrate concentrations. Grass and Forage
793   Science 64, 187–195.
794 Heide, O.M., 1982. Effects of photoperiod and temperature on growth and flowering in
795   Norwegian and British timothy cultivars (Phleum pratense L.). Acta Agriculturae Scandinavia
796   Section B, Soil and Plant Science 32, 241- 252.
797 Heide, O.M., 1994. Control of flowering and reproduction in temperate grasses. New Phytologist
798   128, 347-362.
799 Höglind, M., Schapendonk, A.H.C.M, Van Oijen, M., 2001. Timothy growth in Scandinavia:
800   combining quantitative information and simulation modelling. New Phytologist 151, 355-367.
801 Höglind, M., Hanslin, H.M., Van Oijen, M., 2005. Tillering, leaf area dynamics and regrowth of
802   timothy swards cut at two growth stages. Field Crops Research 93, 51–63.
803 Höglind, M., Jørgensen, M., Østrem, L., 2006. Growth and development of frost tolerance in
804   eight contrasting cultivars of timothy and perennial ryegrass during winter in Norway. In:
805   Proceedings of the NJF Seminar 384, 10–12 August 2006, Akureyri, Iceland, pp. 50–53.
806 Höglind, M., Bakken, A.K., Jørgensen, M., Østrem, L., 2010. Tolerance to frost and ice
807   encasement in cultivars of timothy and perennial ryegrass during winter, Grass For. Sci. 65,
808   431-445.
809 Höglind, M., Hanslin, H.M., Mortensen, L.M., 2011. Photosynthesis and growth of Lolium
810   perenne L. at low irradiance and temperatures in short photoperiods. Environmental and
811   Experimental Botany 70, 297-304.
812 Höglind, M., Thorsen, S.M., Semenov, M.A., 2013. Assessing uncertainties in impact of climate
813   change on grass production in Northern Europe using ensembles of global climate models.
814   Agricultural and Forest Meteorology 170, 103–113.
815 Iwata, Y., Hayashi, M., Hirota, T., 2008. Comparison of snowmelt infiltration under different
816   soil-freezing conditions influenced by snow cover. Vadose Zone Journal 7, 79–86.
817 Jégo, G., Bélanger, G., Tremblay, G.F., Jing, Q., Baron, V.S. 2013. Calibration and performance
818   evaluation of the STICS crop model for simulating timothy growth and nutritive value.",
819   Field Crops Research, 151, 65-77.
820 Jégo, G., Chantigny, M., Pattey, E., Bélanger, G., Rochette, P., Vanasse, A., Goyer, C. 2014.
821   Improved snow-cover model for multi-annual simulations with the STICS crop model under
822   cold, humid continental climates. Agricultural and Forest Meteorology195–196, 38–51.

823   Jing, Q., Bélanger, G., Qian, B., Baron, V. , 2014. Timothy yield and nutritive value with a
824       three-harvest system under the projected future climate in Canada. Canadian Journal of Plant
825       Science 94, 213–222.
826   Larsen, A., 1994. Breeding winter hardy grasses. Euphytica 77, 231-237.
827   Mahfoozi, S.,Limin, A.E., Fowler, D.B., 2001 Developmental regulation of low-temperature
828       tolerance in winter wheat, Ann. Bot. 87, 751-757
829   Matsumoto, N., 2009. Snow moulds: a group of fungi that thrives under snow. Microbes and
830       Environments 1, 14-20.
831   Metropolis, N., Rosenbluth, A.W., Rosenbluth, M.N., Teller, A.H., Teller, E., 1953. Equation of
832       state calculations by fast computing machines. Journal of Chemical Physics 21, 1087-1092.
833   Peacock, J.M., 1976. Temperature and leaf growth in four grass species. Journal of Applied
834       Ecology 13, 225 –232.
835   Persson, T., Höglind, M., 2014. Impact of climate change on harvest security and biomass yield
836       of two timothy ley harvesting systems in Norway. The Journal of Agricultural Science 152,
837       205-216.
838   Persson, T., Höglind, M., Gustavsson, A.M., Halling, M., Jauhiainen, L., Niemeläinen, O.,
839       Thorvaldsson, G., Virkajärvi, P., 2014 Evaluation of the LINGRA timothy model under
840       Nordic conditions. Field Crops Research 161:87-97
841   Rapacz, M., Ergon, Å., Höglind, M., Jørgensen, M. Jurczyk, B., Østrem, L., Rognli, O.A.,
842       Tronsmo, A.M., 2014. Overwintering of herbaceous plants in a changing climate – still more
843       questions than answers. Plant Science 225, 34–44.
844   Riedo, M., Grub, A., Rosset M., Fuhrer, J. ,1998. A pasture simulation model for dry matter
845       production and fluxes of carbon, nitrogen, water and energy. Ecological Modelling 105, 141-
846       183.
847   Riedo, M., Gyalistras, D., Fischlin, A., Rosset, M., Fuhrer J., 1999. Using an ecosystem model
848       linked to GCM-derived local weather scenarios to analyse effects of climate change and
849       elevated CO2 on dry matter production and partitioning, and water use in temperate managed
850       grasslands. Global Change Biology 5, 213–223
851   Rodriguez, D., Van Oijen, M., Schapendonk, A.H.C.M., 1999. LINGRA-CC: a sink-source
852       model to simulate the impact of climate change and management on grassland productivity.
853       New Phytologist 144, 359–368.
854   Schapendonk, A.H.C.M., Stol ,W., Van Kraalingen, D.W.G., Bouman, B.A.M.1998. LINGRA, a
855       sink/source model to simulate grassland productivity in Europe. European Journal of
856       Agronemy 9, 87-100.

857   Seppänen, M., Pakarinen, K., Jokela, V., Andersen, J., Fiil, A., Santanen, A., Virkajärvi, P.,
858       2010. Vernalization response of Phleum pratense L. and its relationship to canopy
859       architecture, stem morphology and expression of VRN1 and VRN2, Ann. Bot. 106, 697-707.
860   Sunde, M., 1996. Effects of winter climateongrowth potential, carbohydrate content and cold
861       hardiness of timothy (Phleum pratence L.) and red clover (Trifolium pratence L.). Ph.D.
862       thesis, Agricultural University of Norway.
863   Thorsen, S.M., Roer, A.G., Van Oijen, M., 2010. Modelling the dynamics of snow cover, soil
864       frost and surface ice in Norwegian grasslands. Polar Research 29, 110-126.
865   Thorsen, S.M., Höglind, M., 2010. Modelling cold acclimation and de-acclimation in timothy.
866       Sensitivity analysis and Bayesian calibration. Agricultural and Forest Meteorology 150: 1529-
867       1542.
868   Thornley, J.H.M., Cannell, M.G.R., 1997. Temperate grassland responses to climate change: an
869       analysis using the Hurley Pasture Model. Annals of Botany 80, 205–221.
870   Tronsmo A.M. 1984. Predisposing effects of low temperatures on resistance to snow mould
871       fungi. Acta Agriculturae Scandinavica 34, 210-220.
872   Tubiello, F.N., Soussana, J.-F., S. Howden, M.  2007. Crop and pasture response to climate
873       change. Proceedings of the National Academy of Sciences 104, 19686-19690.
874   Van Oijen, M., Höglind, M., Hanslin, H.M., Caldwell, N., 2005a. Process-based modeling of
875       timothy regrowth. Agronomy Journal 97, 1295-1303.
876   Van Oijen, M., Rougier, J., Smith, R,  2005b. Bayesian calibration of process-based forest
877       models: bridging the gap between models and data. Tree Physiology 25, 915-927.
878   Van Oijen, M., Reyer, C., Bohn, F.J., Cameron, D.R., Deckmyn, G., Flechsig, M., Härkönen, S.,
879       Hartig, F., Huth, A., Kiviste, A., Lasch, P., Mäkelä, A., Mette, T., Minunno, F., Rammer, W.,
880       2013. Bayesian calibration, comparison and averaging of six forest models, using data from
881       Scots pine stands across Europe. Forest Ecology and Management 289, 255-268.
882   Van Oijen, M., Höglind, M., Cameron, D.R., Thorsen, S.M. 2015. BASGRA_2014.
883           http://dx.doi.org/10.5281/zenodo.27867 .
884   Van Oijen, M., Höglind, M. 2016. Toward a Bayesian procedure for using process-based models
885       in plant breeding, with application to ideotype design. Euphytica 207, 627-643.